

# RSC Advances



This is an *Accepted Manuscript*, which has been through the Royal Society of Chemistry peer review process and has been accepted for publication.

*Accepted Manuscripts* are published online shortly after acceptance, before technical editing, formatting and proof reading. Using this free service, authors can make their results available to the community, in citable form, before we publish the edited article. This *Accepted Manuscript* will be replaced by the edited, formatted and paginated article as soon as this is available.

You can find more information about *Accepted Manuscripts* in the [Information for Authors](#).

Please note that technical editing may introduce minor changes to the text and/or graphics, which may alter content. The journal's standard [Terms & Conditions](#) and the [Ethical guidelines](#) still apply. In no event shall the Royal Society of Chemistry be held responsible for any errors or omissions in this *Accepted Manuscript* or any consequences arising from the use of any information it contains.

**Temperature effects on arsenate adsorption onto goethite and its preliminary application to arsenate removal from simulative geothermal water**

Linlin Hao<sup>a,b</sup>, Tong Ouyang<sup>a,\*</sup>, Limin Lai<sup>a</sup>, Yao-Xing Liu<sup>c</sup>, Shanshan Chen<sup>a</sup>, Hongyou Hu<sup>a,\*</sup>, Chang-Tang Chang<sup>d</sup>, Juan-Juan Wang<sup>a</sup>

<sup>a</sup> Department of Environmental Science and Technology, College of the Environment and Ecology, and Key Laboratory of the Ministry of Education for Coastal and Wetland Ecosystem, Xiamen University, Xiang'an South Road, Xiang'an District, Xiamen 361102, China

<sup>b</sup> State Key Laboratory of Urban Water Resource and Environment, School of Municipal and Environmental Engineering, Harbin Institute of Technology, Harbin 150090, China

<sup>c</sup> College of Hydraulic and Environmental Engineering, China Three Gorges University, Yichang 443002, China

<sup>d</sup> Department of Environmental Engineering, National ILAN University, I-Lan 26041, Taiwan

\* Corresponding authors: Phone: +865922181613, Fax: +865922185889, E-mail address: yz3t@xmu.edu.cn (T. Ouyang); Phone: +865922880233, Fax: +865922185889, E-mail address: hongyouhu@xmu.edu.cn (H.-Y. Hu).

## Abstract

Laboratory batch experiments were conducted in order to assess the performance of goethite in removing arsenate from water regarding the impacts of temperature. All batch experiments were conducted at four temperatures (30, 50, 70 and 90°C) at pH 4.6. Results showed that both the uptake rate and capacities were significantly enhanced with the temperature increasing from 30 to 90°C. The adsorption kinetics followed a Pseudo-second-order model with the coefficients of Determination ( $R^2$ ) all above 0.999. The process followed the Langmuir model and several thermodynamic parameters were calculated. Arsenate adsorption was facilitated under simulative geothermal water condition than RO (Reverse Osmosis) water. The crystallite structure of goethite was not changed after adsorption at various temperatures. XPS results showed the decrease of the content of iron hydroxyl group, which demonstrated that arsenate adsorption onto goethite may be realized through the replacement of the iron hydroxyl group to form inner-sphere bidentate/monedentate complex at pH 4.6.

**Keywords:** Goethite; Arsenic (As(III)/As(V)); Adsorption; Simulative geothermal water;

## 1. Introduction

Geothermal water as a kind of natural resource has been used for human people for a long time. The importance of geothermal water has increased over the last decade as demand for non-fossil fuel energy sources has expanded. <sup>1</sup> Like a double-edged sword, the significant environmental changes such as surface disturbances, thermal effects and emissions of contaminants are also brought by geothermal utilization. <sup>2</sup> The main potential pollutants in geothermal discharged waters are hydrogen sulphide, mercury,

arsenic and other trace metals.<sup>3</sup>

Arsenic in geothermal water is detected at an elevated concentration in many places of the world such as the Tibet yangbajain geothermal fields, the southeast coastal area of China mainland, Taiwan and so on.<sup>4</sup> Thompson and Demonge reported that Geothermal water in Yellowstone National Park contained high concentrations of As 1~7800 µg/L.<sup>5</sup> The Rio Loa basin El Tatio geothermal field of Chile was reported to have very high arsenic concentration values up to 27.0 mg/L, Los Humeros geothermal field of Mexico was even reported to have the arsenic concentration as high as 73.6 mg/L.<sup>6</sup> Natural geothermal water (including thermal spring water) was increasingly reported to be high levels of arsenic, and this phenomenon was frequently found in Southeast of China and Taiwan area. Many of the arsenic-containing geothermal water are discharged directly into nature without treatment, so lots of environmental problems and potential problems are triggered.

The distribution of As(III)/As(V) is influenced by pH and redox conditions, As(III) is more toxic than As(V), the World Health Organization have lowered the maximum contaminant level of total arsenic in drinking water to 10 µg/L. Mobility and transformation of As-tainted geothermal water have become significant concerns worldwide in environmental health. The final fate of arsenic in geothermal water rises to the earth's surface and there is concern that it may contaminate the related groundwater systems, surface-water systems and soil systems.<sup>7</sup>

There are various kinds of iron oxides and oxyhydroxides existing in soils, sediments and aquatic environments such as goethite ( $\alpha$ -FeOOH), lepidocrocite

( $\gamma$ -FeOOH), hematite ( $\alpha$ -Fe<sub>2</sub>O<sub>3</sub>) and so on.<sup>8</sup> A great variety of iron oxides and oxyhydroxides usually have a strong affinity for arsenic species.<sup>9,10</sup> In this study, goethite is selected as the presentative iron oxyhydroxide because it is widespread in soil system and is a primary component of soil.<sup>11</sup> Investigating the reactions between goethite and different arsenic species is important for providing insight into the rule of Mobility& transformation of arsenic in geothermal water.

So far, many studies focus on arsenic adsorption onto goethite.<sup>12, 13</sup> However, a review of the literatures showed that little has been done to determine the impacts of temperature on the adsorption process. So we conduct a detailed study in a batch system in order to gain an understanding of the effects of temperature on arsenate adsorption onto goethite and the adsorption performance under simulative geothermal water condition.

This paper focused on the temperature effect on arsenate adsorption onto goethite, because the temperature is the first consideration of geothermal water. Previous papers usually investigated the temperature effect between 20 and 60°C,<sup>14-16</sup> we further considered the comparatively higher temperature 70 and 90°C, because we have detected the temperature of thermal spring water near Xiamen city (Fujian province, China) was 88°C. The pH was adjusted to 4.6 with reference from Taiwan Datun volcanic region hot springs reported by Chen Bochun et al.<sup>17</sup> that the pH was appeared to be acidic around 4.6, some hot springs in Taiwan are even as low as 1~2. Usually the pH values of the acidic geothermal discharged water fall in between 4~5.

## 2. Materials and methods

## 2.1 Materials

The granular goethite ( $\alpha$ -FeOOH) in this study is synthesized in the laboratory. Solution of 1 M  $\text{Fe}(\text{NO}_3)_3$  is adjusted to pH 11.0 and stirred in a water bath at  $70 \pm 1^\circ\text{C}$  for 24 h, the suspension is purged with  $\text{N}_2$  to remove  $\text{CO}_2$ , then adjust the temperature to  $90^\circ\text{C}$  for heating 72 h followed by repeated rinsing of the solids with deionized water, the solution with very high concentration of solids is ultrasonically dispersed for 30 min with adding small amount of absolute ethyl alcohol, finally we get the granular goethite through freeze drying technique process. The product is stored at  $4^\circ\text{C}$  for subsequent use.

The As(V) stock solutions are prepared by  $\text{Na}_2\text{HAsO}_4 \cdot 7\text{H}_2\text{O}$  (AR). All the chemicals used in the experiments are AR grade.

## 2.2 Batch sorption

The adsorption experiments are performed with a background electrolyte of 0.01 M  $\text{NaNO}_3$ , suspensions of goethite are made by adding 0.05 g goethite solids to 100 mL of 0.01 M  $\text{NaNO}_3$  and are continuously mixed on a magnetic stirring apparatus at temperature  $30^\circ\text{C}$  for 2 h to make the surface of goethite reach equilibrium, the pH of the arsenic stock solutions and goethite solutions are adjusted to  $4.6 \pm 0.2$  using dilute  $\text{HNO}_3$  and  $\text{NaOH}$  solutions.

Adsorption isotherms process is conducted in a shaking water bath with a temperature controller. Batch tests are performed in 200 mL bottles containing 0.5 g/L goethite and are equilibrated with 1, 2, 5, 10, 15, 20, 30, 40, 50 mg/L As(V) shaking at 150 rpm for 24 h at 30, 50, 70,  $90^\circ\text{C}$  respectively. Finally the suspensions are filtered through a  $0.22 \mu\text{m}$  membrane filter.

The kinetics experiments are conducted in a closed system consisting of a double-layer round glass reactor that is placed on a magnetic stirring apparatus, the double-layer round glass reactor is connected with a thermostat water bath which could be adjusted to different temperatures, the water flows through the inside of the double-layer glass reactor to keep the temperature constant. A pH electrode combined with a thermometer is inserted below the surface of solution to detect the pH change in the reactor. The initial As(V) concentration is 1 mg/L and the goethite suspensions are 0.2 g/L. The schematic diagram of experimental apparatus for kinetic study was shown in Fig. S1.

### 2.3 Characterizations

The morphology of goethite was monitored with SEM (Scanning electron microscopy), using a JEOL scanning electron microscope model Hitachi S-4800. XRD (Powder X-ray diffraction) data were collected from  $10^\circ$  to  $70^\circ$   $2\theta$  by using Cu  $K_\alpha$  ( $\lambda=0.15418$  nm) incident radiation in a PANalytical X'pert PRO diffractometer. XPS (X-ray photoelectron spectroscopy) data were collected on a PHI QUANTUM 2000 spectrometer (PHI, USA) with monochromatic Al K $\alpha$  radiation (1486.6 eV).

The arsenic analytical method is hydride generation atomic fluorescence spectroscopy (HG-AFS), capable of detecting arsenic as low as 1.0  $\mu\text{g/L}$ . All the samples were pre-reduced by 5% (w) thiourea - 5% (w) ascorbic acid to ensure all the arsenic species are converted to detectable As(III).

## 3. Results and discussion

### 3.1 Granular goethite characterization

The SEM images are shown in Fig. 1 (a), goethite prepared in this study form rodlike nanoparticles which are aggregated together. The specific surface area of the goethite samples is determined by the N<sub>2</sub>/BET method to be 106.6±1 m<sup>2</sup>/g. The structure analysis by XRD (as in Fig. 1 (b)) demonstrates that the granular iron oxyhydroxide is goethite compared with the standard XRD pattern (JCPDS 29-0713) of pure goethite.

### 3.2 Adsorption kinetics

The effect of time on the arsenate uptake rate at different temperatures is shown in Fig. 2, which shows a rapid initial uptake followed by a slow approach to equilibrium. Initial rapid adsorption rate can be attributed to the more adsorption sites at the initial stage, the arsenic species can interact easily with the sites. The slower adsorption may be due to slower diffusion into the interior of goethite and the decrease of the driving concentration between bulk solution and goethite surface. The adsorption achieves equilibrium gradually within 100 min at 30, 50, 70, 90°C. With temperature increased from 30°C to 70°C, the slopes of kinetic curves (initial rapid stage) gradually became steeper, indicating the higher temperature accelerated the reaction rate. When temperature was increased from 70°C to 90°C, a trend of increase was also observed but the growth rate became smaller compared with 30 to 70°C. It may indicated that arsenate adsorption onto goethite became less sensitive to temperature within 70~90°C.

Several kinetic models, i.e. pseudo-second-order, Elovich equation, Intraparticle diffusion equations are used to fit the kinetics data.<sup>18</sup> The calculated parameters of the three kinetic models were listed in Table. 1 and the fitting curves of Elovich equation, Intraparticle diffusion models were shown in Fig. S2.



The pseudo-second-order equation could be written as:

$$\frac{t}{q_t} = \frac{1}{k_2 q_e^2} + \frac{1}{q_e} t \quad (1)$$

and the Intraparticle diffusion equation:

$$q_t = k_d t^{1/2} + C \quad (2)$$

Where  $t$  is time, and  $q_t$  is the adsorption capacity at  $t$ ,  $q_e$  is the equilibrium adsorption capacity.  $k_1$ ,  $k_2$ ,  $k_d$  are rate constants of the pseudo-first-order, pseudo-second-order and Intraparticle diffusion equations, respectively. Which are strongly depended on the applied operating conditions such as the initial solute concentration, pH, temperature and so on.

A simple modified Elovich equation is as follows:

$$q_t = \left(\frac{1}{\beta}\right) \ln(\alpha\beta) + \left(\frac{1}{\beta}\right) \ln t \quad (3)$$

Where  $\alpha$  and  $\beta$  are constants,  $t$  is the time, and  $q_t$  is adsorption capacity at  $t$ . Elovich equation is frequently used to describe the initial time period of sorption process when the system is relatively far from equilibrium.<sup>19</sup> This model has been proven to be suitable for the heterogeneous systems, which might exhibit different activation energies for the chemical adsorption on the surface.<sup>20</sup>

The adsorption process on porous adsorbents are generally described with four stages, bulk diffusion, film diffusion, intraparticle diffusion and adsorption at a special site on the surface. Bulk and film diffusion are generally assumed to be rapid because of the agitation condition. As can be seen from Table 1, the pseudo-second-order could well describe the experimental data with the linear regression coefficients ( $R^2$ ) all above 0.999,

indicating that arsenate adsorption onto goethite was second-order chemical adsorption process. To better understand the rate-determining step of adsorption, the kinetic data were tested using the Intraparticle diffusion equation. As shown in Fig. S1, the fitting curves were apparently divided into two stages, which were separately linearly fitted well with the Intraparticle diffusion model, indicating the intraparticle diffusion process is a key rate-limiting step. According to the research of Barrow,<sup>21</sup> goethite surfaces are variable and possibly composed of many crystal defects and micropores, the diffusion process may be attributed to these areas.<sup>22</sup> The initial rapid stage of kinetic curves was fitted with Elovich equation, the values of correlation coefficients  $R^2$  are greater than 0.93 at four temperatures. Good conformation to Elovich equation suggested the nature of monolayer chemical adsorption.

### 3.3 Adsorption isotherms

The adsorption isotherms of arsenate at pH 4.6 with ionic strength of 0.01 mol/L  $\text{NaNO}_3$  were presented in Fig. 3, the adsorption capacity increased with an increase of initial arsenic concentration. Adsorption capacity as well increased from 19.84 mg/g to 25.97 mg/g with a rise in temperature from 30 to 70°C. However, smaller difference of adsorption capacities (25.97 to 26.60 mg/g) were observed with the temperature increased from 70 to 90°C, which was in agreement with the kinetic results. At pH 4.6, As(V) exhibits the negative charged  $\text{H}_2\text{AsO}_4^-$  while the surface of goethite is positive charged with the key function group of  $-\text{FeOH}_2^+$ ,<sup>23</sup> anionic arsenate adsorption is probably enhanced by Coulombic attractions.<sup>24</sup>

The isotherms are fitted with Freundlich and Langmuir equations, the parameters

were summarized in Table 2. The linear regression coefficients of Langmuir model are all above 0.995, suggesting the identical adsorption sites of goethite surface and the nature of monolayer adsorption. The isotherms were also well described by Freundlich model. According to C-H.Yang,<sup>25</sup> The Freundlich model was set up with emphasis on two factors, the lateral interaction among the adsorbed molecules and the heterogeneity of the energetic surface. Besides, the Freundlich model was often applied to the situation when the initial concentration of the adsorbate is relatively low.<sup>26</sup>

The Langmuir isotherm equation, as indicated below:

$$\frac{C_e}{q_e} = \frac{C_e}{q_{\max}} + \frac{1}{q_{\max} K_L} \quad (4)$$

Where,  $q_e$  is the quantity of the species adsorbed at equilibrium (mg/g),  $K_L$  is a constant representing the virtual bonding strength between the target species and adsorber,  $C_e$  is the equilibrium concentration of adsorbate in the solution,  $q_{\max}$  is the maximum loading of the adsorbate onto adsorbent.

The Freundlich isotherm equation was expressed as follows:

$$\ln q_e = \ln K_F + 1/n \ln C_e \quad (5)$$

Where,  $q_e$  is the quantity of the species adsorbed at equilibrium (mg/g),  $K_F$  is a constant which is a measure of sorption capacity,  $1/n$  is a measure of adsorption density,  $C_e$  is the equilibrium concentration of adsorbate in the solution.

As shown in Table 2, the values of  $K_L$  for arsenate adsorption increased from 0.446 to 1.001 with the temperature increasing from 30 to 90°C, which was in good agreement with the observation that adsorption process was promoted by increasing of temperature. The values of  $1/n$  (0.233~0.338) between 0 and 1 represent a favorable adsorption of

arsenate onto goethite.

### 3.4 Calculation of thermodynamic parameters

The temperature dependence of arsenic adsorption is associated with changes in several thermodynamic parameters such as  $\Delta G^\circ$  (the standard Gibbs free energy change),  $\Delta H^\circ$  (enthalpy change),  $\Delta S^\circ$  (entropy change), the parameters are calculated by using equations below:

$$\ln(K_0) = \Delta S^\circ/R - \Delta H^\circ/RT \quad (6)$$

$$\Delta G^\circ = -RT \cdot \ln(K_0) \quad (7)$$

where,  $R$  is the universal gas constant,  $T$  is temperature (K) and  $K_0$  is the thermodynamic equilibrium constant,  $K_0$  is determined using the method of Karthikeyan<sup>27</sup> by plotting  $\ln(q_e/C_e)$  versus  $q_e$  and extrapolating to zero  $\ln(q_e/C_e)$  (Fig. S3).

As shown in Table. 3, the values of  $\Delta G^\circ$  are calculated from equation (7), the values of  $\Delta H^\circ$  and  $\Delta S^\circ$  are calculated from the slope and intercept of Van't Hoff plot. The positive value of  $\Delta H^\circ$  (11.29 kJ/mol) and negative values of  $\Delta G^\circ$  (-3.31 ~ -6.31 kJ/mol) confirm the spontaneous and endothermic nature of adsorption process, and the decrease of  $\Delta G^\circ$  with a rise in temperature suggests the stronger affinity at higher temperatures. The positive value of  $\Delta S^\circ$  implies an increase of randomness at the solid/solution interface.

### 3.5 Adsorption under simulative geothermal water conditions

The components of various kinds of geothermal water differ from each other, so modeling of such system is very challenging. The simulative geothermal water was prepared with reference to the components of Datun volcanic region hot springs in

Taiwan reported by Chen Bochun et al.<sup>17</sup> The detailed components of simulative geothermal water were listed on the Table 4. As can be seen from Fig. 4, simulative geothermal water with multiple co-existing components promoted the adsorption of As(V), indicating that certain concentrations of ionic strength were beneficial for arsenate adsorption onto goethite. The maximum adsorption capacity was increased from 21.7 to 27.1 mg/g, which was probably due to the effect of compression of double charged layer and be favorable for the arsenic species to get closer to the goethite surface. Multivalent cations such as  $\text{Ca}^{2+}$ ,  $\text{Mg}^{2+}$ ,  $\text{Fe}^{3+}$  are probably going to form co-precipitation ( $\text{CaHAsO}_4$ ,  $\text{MgHAsO}_4$ ,  $\text{FeAsO}_4 \cdot 2\text{H}_2\text{O}$ ) with arsenate, thereby improving arsenate removal efficiency. So adsorption experiments in simulating geothermal water (lacking  $\text{Ca}^{2+}$ ,  $\text{Mg}^{2+}$ ,  $\text{Fe}^{3+}$ ,  $\text{Al}^{3+}$ ) were carried out in this study. The results show that arsenate adsorption in simulative geothermal water are still enhanced compared with that in simulative geothermal water (lacking  $\text{Ca}^{2+}$ ,  $\text{Mg}^{2+}$ ,  $\text{Fe}^{3+}$ ,  $\text{Al}^{3+}$ ), indicating that multivalent cations such as  $\text{Ca}^{2+}$ ,  $\text{Mg}^{2+}$ ,  $\text{Al}^{3+}$  promote the As(V) adsorption process. The result is similar with the testing result of M. Stachowicz<sup>28</sup> that both  $\text{Ca}^{2+}$  and  $\text{Mg}^{2+}$  promoted  $\text{PO}_4^{3-}$  adsorption onto goethite.

Many competitive anions were reported to have adverse effect on arsenic adsorption onto goethite, the main single interfering ion (phosphate and fluorin) are carried out by taking equal concentrations of the competing anion as that of arsenic, results showed that phosphate had a profound competing impact on arsenic adsorption, this is not difficult to understand because elements of Phosphorus and arsenic are in the same main group and  $\text{PO}_4^{3-}$ ,  $\text{AsO}_4^{3-}$  have the identical chemical structure, both molecules are tetrahedral oxyanions with similar  $\text{pK}_a$  values.<sup>29</sup> Moreover, fluorin is frequently detected at high

concentrations in geothermal water, our results showed that fluorine had little interfering effect on arsenate adsorption as shown in Fig. S4.

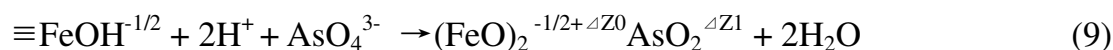
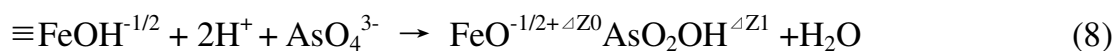
### 3.6 Analysis of XRD and XPS spectra

The crystallite structure of goethite after arsenate adsorption (initial arsenic solution is 10 mg/L) at four different temperatures are investigated. Fig. 5 shows the XRD patterns of goethite at four temperatures, all the XRD patterns are consistent with that of standard XRD card (JCPDS 29-0713), it was demonstrated that goethite could exist stably even at temperature as high as 90°C, and the crystallite structure of goethite is not changed after arsenic species adsorption.

To prove the existence of arsenic onto goethite, XPS analysis is conducted for the sample of goethite reacted with arsenate. Fig. 6 illustrated the wide scan XPS spectrum of goethite after arsenate adsorption. The occurrence of new peaks for arsenate of As1s and As3d were observed, confirming the adsorption of arsenate onto goethite. Fig. S5 exhibited the values of the binding energy of the As3d core level in arsenic oxides are ca. 45.5 eV for As(V). Therefore, it can be demonstrated that the valence state of As(V) was not changed during the adsorption process.

To further investigate the surface hydroxyl group of goethite, O(1s) narrow scans of goethite before and after As(V) adsorption are analysed. The O(1s) spectrum is composed of overlapped peaks of oxide oxygen ( $O^{2-}$ ), hydroxyl ( $OH^-$ ), and sorbed water ( $H_2O$ ).<sup>30</sup> The O(1s) peaks are fitted with two components ( $O^{2-}$  at 529.6 eV and  $OH^-$  at 530.9 eV) for pure  $\alpha$ -FeOOH, an additional peak at 531.3 eV can be attributed to the absorbed  $H_2O$ .

All of the spectra are fitted using a 50:50 Gaussian:Lorentzian peak shape and the fitting results are obtained as shown in Fig. 7 and Fig. 8. The key reactive group of  $\text{OH}^-$  occupies 37.4% of the surface oxygen in goethite as shown in Fig. 7, a significant decrease of the  $\text{OH}^-$  species was observed after arsenate adsorption at different temperatures, occupying 25.6%, 24.5%, 23.9% and 23.6% at 30°C, 50°C, 70°C and 90°C, respectively, as shown in Fig. 8. This result might indicate that singly coordinated iron hydroxyl ( $\text{OH}^-$ ) was involved and replaced with arsenate oxyanion, the reaction was probably carried out through the formation of inner-sphere monodentate complex  $\text{FeOAsO}_2\text{OH}$  and inner-sphere bidentate complex  $(\text{FeO})_2\text{AsO}_2$ , which was in accordance with the possible reactions shown below.<sup>28</sup>



$\Delta Z_0$ ,  $\Delta Z_1$  are the interfacial charge distribution (CD) model coefficients,  $\Delta Z_0 + \Delta Z_1$  is equal to the charge introduced by arsenate adsorption.

#### 4. Conclusions

The present study showed that the synthesized goethite has a strong affinity for inorganic arsenate in aqueous system, temperature plays an important role in the arsenic species adsorption, the adsorption capacities increase with an increase in temperature 30~90°C. Adsorption isotherms could be fitted well to Langmuir model and the kinetics fit best to the pseudo-second equation. Adsorption of arsenate exhibited a better performance under simulative geothermal water conditions, co-existing multivalent cations such as  $\text{Ca}^{2+}$ ,  $\text{Mg}^{2+}$ ,  $\text{Al}^{3+}$  facilitated arsenate adsorption. XRD analysis revealed

that the crystallite structure of goethite after arsenate adsorption was not changed within temperature 30~90°C. The content of iron hydroxyl group decreased from 35.4% of the raw goethite to 25.6% at 30°C and 23.2% at 90°C after adsorption, which indicated that the singly coordinated iron hydroxyl ( $\text{OH}^-$ ) was involved and higher temperature (50-90°C of geothermal water) facilitated arsenate to form the inner-sphere bidentate or monodentate complex at pH 4.6.

### Acknowledgement

This research is financially supported by the National Natural Science Foundation of China (Contract No. 21077086). The authors would like to thank all the reviewers for their helpful comments and valuable suggestions.

### References

- 1 G. Axelsson, *Geothermics.*, 2010, **39**, 283-291.
- 2 L. Paoli, S. Loppi, *Environ. pollut.*, 2008, **155**, 383-388.
- 3 S. Loppi, L. Paoli, C. Gaggi, *J. Atmos. Chem.*, 2006, **53**, 93-105.
- 4 K. Tyrovola, N.P. Nikolaidis, N. Veranis, N. Kallithrakas-Kontos, P.E. Koulouridakis, *Water Res.*, 2006, **40**, 2375-2386.
- 5 B. Planer-Friedrich, J. London, R.B. McCleskey, D.K. Nordstrom, D. Wallschläger, *Environ. Sci. Technol.*, 2007, **41**, 5245-5251.
- 6 P. Smedley, D. Kinniburgh, *Appl. Geochem.*, 2002, **17**, 517-568.
- 7 À. Piqué, F. Grandia, À. Canals, *Water Res.*, 2010, **44**, 5618-5630.
- 8 R.V. Morris, H.V. Lauer, C.A. Lawson, E.K. Gibson, G.A. Nace, C. Stewart, *J. Geo-phys. Res: Solid Earth (1978–2012).*, 1985, **90**, 3126-3144.



- 9 Y. Mamindy-Pajany, C. Hurel, N. Marmier, M. Roméo, *Desalination.*, 2011, **281**, 93-99.
- 10 S.K. Maji, Y.-H. Kao, C.-W. Liu, *Desalination.*, 2011, **280**, 72-79.
- 11 W. Hartley, R. Edwards, N.W. Lepp, *Environ. pollut.*, 2004, **131**, 495-504.
- 12 Y. Mamindy-Pajany, C. Hurel, N. Marmier, *C. R. Chim.*, 2009, **12**, 876-881.
- 13 T.S. Choong, T. Chuah, Y. Robiah, F. Gregory Koay, I. Azni, *Desalination.*, 2007, **217**, 139-166.
- 14 K. Banerjee, G. L. Amy, M. Prevost, S. Nour, M. Jekel, P. M. Gallagher, C. D. Blumenschein, *Water Res.*, 2008, **42**, 3371-3378.
- 15 F. Partey, D. Norman, S. Ndur, R. Nartey, *J. Colloid Interface Sci.*, 2008, **321**, 493-500.
- 16 S. Kundu, A. K. Gupta, *Colloids and Surfaces A: Physicochemical and Engineering Aspects.*, 2006, **273**, 121-128.
- 17 B.C. Chen, Taiwan joint academic symposium on earth science[C], 2007, 125-128.
- 18 D. Bulgariu, L. Bulgariu, *Bioresour. Tech.*, 2012, **103**, 489-493.
- 19 W. Plazinski, W. Rudzinski, A. Plazinska, *Advan. Coll. Interface Sci.*, 2009, **152**, 2-13.
- 20 S. Fendorf, M.J. Eick, P. Grossl, D.L. Sparks, *Environ. Sci. Technol.*, 1997, **31**, 315-320.
- 21 N. Barrow, G. Brümmer, L. Fischer, *Eur. J. Soil Sci.*, 2012, **63**, 389-398.
- 22 H. Liu, T. Chen, R.L. Frost, *Chemos.*, 2014, **103**, 1-11.
- 23 P. Lakshminathiraj, B. Narasimhan, S. Prabhakar, G. Bhaskar Raju, *J. Hazard. Mater.*, 2006, **136**, 281-287.
- 24 C. Su, R.W. Puls, *Environ. Sci. Technol.*, 2001, **35**, 1487-1492.
- 25 C.H. Yang, *J. Colloid Interface Sci.*, 1998, **208**, 379-387.
- 26 J. Zhang, R. Stanforth, *Langmuir.*, 2005, **21**, 2895-2901.
- 27 G. Karthikeyan, K. Anbalagan, N.M. Andal, *J. Chem. Sci.*, 2004, **116**, 119-127.

- 28 M. Stachowicz, T. Hiemstra, W.H. van Riemsdijk, *J. Colloid Interface Sci.*, 2008, **320**, 400-414.
- 29 F. Kolbe, H. Weiss, P. Morgenstern, R. Wennrich, W. Lorenz, K. Schurk, H. Stanjek, B. Daus, *J. Colloid Interface Sci.*, 2011, **45**, 565-571.
- 30 Y. Zhang, M. Yang, X.M. Dou, H. He, D.S. Wang, *Environ. Sci. Technol.*, 2005, 39, 7246-7253.
- 31 Z. Sun, X. Feng, W. Hou, *Nanotech.*, 2007, **18**, 455-607.

Table 1. The kinetic models fitting parameters of As(V) adsorption onto goethite at various temperatures at pH 4.6.

| Kinetic models | Pseudo second-order equation                                       |       | Intraparticle diffusion function                                     |       |
|----------------|--|-------|--|-------|
|                | $k_2$<br>( $\text{g} \cdot \text{mg}^{-1} \cdot \text{min}^{-1}$ ) | $R^2$ | $k_d$<br>( $\text{mg} \cdot \text{L}^{-1} \cdot \text{min}^{-1/2}$ ) | $R^2$ |
| Temperature    |  |       |  |       |
| 30°C           | 0.033  | 0.999 | 0.063  | 0.576 |
| 50°C           | 0.043  | 0.999 | 0.055  | 0.461 |
| 70°C           | 0.156  | 0.999 | 0.049  | 0.330 |
| 90°C           | 0.290  | 0.999 | 0.040  | 0.273 |

Table 2. The parameters of adsorption isotherms of As(V) adsorption onto goethite at pH 4.6.

| Temperature (°C) | Langmuir isotherm |              |       | Freundlich isotherm |              |       |
|------------------|-------------------|--------------|-------|---------------------|--------------|-------|
|                  | $Q_{\max}$ (mg/g) | $k_L$ (L/mg) | $R^2$ | $n$                 | $K_F$ (mg/g) | $R^2$ |
| 30               | 19.84             | 0.446        | 0.995 | 2.958               | 6.208        | 0.974 |
| 50               | 22.32             | 0.598        | 0.995 | 3.094               | 7.740        | 0.984 |
| 70               | 25.97             | 0.992        | 0.997 | 3.188               | 10.15        | 0.967 |
| 90               | 26.60             | 1.001        | 0.997 | 4.301               | 13.31        | 0.963 |

Table 3. Thermodynamic parameters for As(V) adsorption onto goethite at different temperatures at pH 4.6.

| Temperature(°C) | $K_0$ | $\Delta G^\circ$ (kJ/mol) | $\Delta S^\circ$ (kJ/mol/K) | $\Delta H^\circ$ (kJ/mol) |
|-----------------|-------|---------------------------|-----------------------------|---------------------------|
| 30              | 3.72  | -3.31                     |                             |                           |
| 50              | 4.57  | -4.08                     |                             |                           |
| 70              | 5.40  | -4.81                     | 0.045                       | 11.29                     |
| 90              | 8.09  | -6.31                     |                             |                           |

Table 4. The components of simulative geothermal water

| Components                     | Concentration (mg/L) |
|--------------------------------|----------------------|
| Mn <sup>2+</sup>               | 1.0                  |
| Mg <sup>2+</sup>               | 1.0                  |
| Al <sup>3+</sup>               | 1.3                  |
| Ca <sup>2+</sup>               | 2.3                  |
| Fe <sup>2+</sup>               | 0.5                  |
| F <sup>-</sup>                 | 2.0                  |
| PO <sub>4</sub> <sup>3-</sup>  | 1.0                  |
| SiO <sub>3</sub> <sup>2-</sup> | 2.6                  |
| NO <sub>3</sub> <sup>-</sup>   | 6.2                  |
| Cl <sup>-</sup>                | 4.4                  |
| SO <sub>4</sub> <sup>2-</sup>  | 17.5                 |
| K <sup>+</sup>                 | 0.5                  |
| Na <sup>+</sup>                | 4.8                  |
| NH <sub>4</sub> <sup>+</sup>   | 0.3                  |

### Figure captions

Fig. 1 (a) SEM images of goethite. (b) The XRD pattern of goethite.

Fig. 2 Kinetics of As(V) adsorption onto goethite at 30, 50, 70, 90°C (As initial concentration 1 mg/L, adsorbent dosage 0.2 g/L, pH 4.6.) and Pseudo-second-order fitting curve.

Fig. 3 Adsorption isotherm for As(V) adsorption onto goethite at 30, 50, 70, 90°C (the initial concentration of As is 1, 2, 5, 10, 20 mg/L, respectively, adsorbent dosage 0.5 g/L, pH 4.6.)

Fig. 4 As(V) adsorption onto goethite under simulative geothermal water conditions at 30, 50, 70, 90°C (the initial As concentration is 20 mg/L, goethite concentration 0.5 g/L, pH 4.6.)

Fig. 5 XRD patterns of goethite and after arsenic adsorption at different temperatures.

Fig. 6 The XPS spectra of wide scan of As-loaded goethite.

Fig. 7 O1s spectra of goethite.

Fig. 8 O1s spectra of goethite after As(V) adsorption.

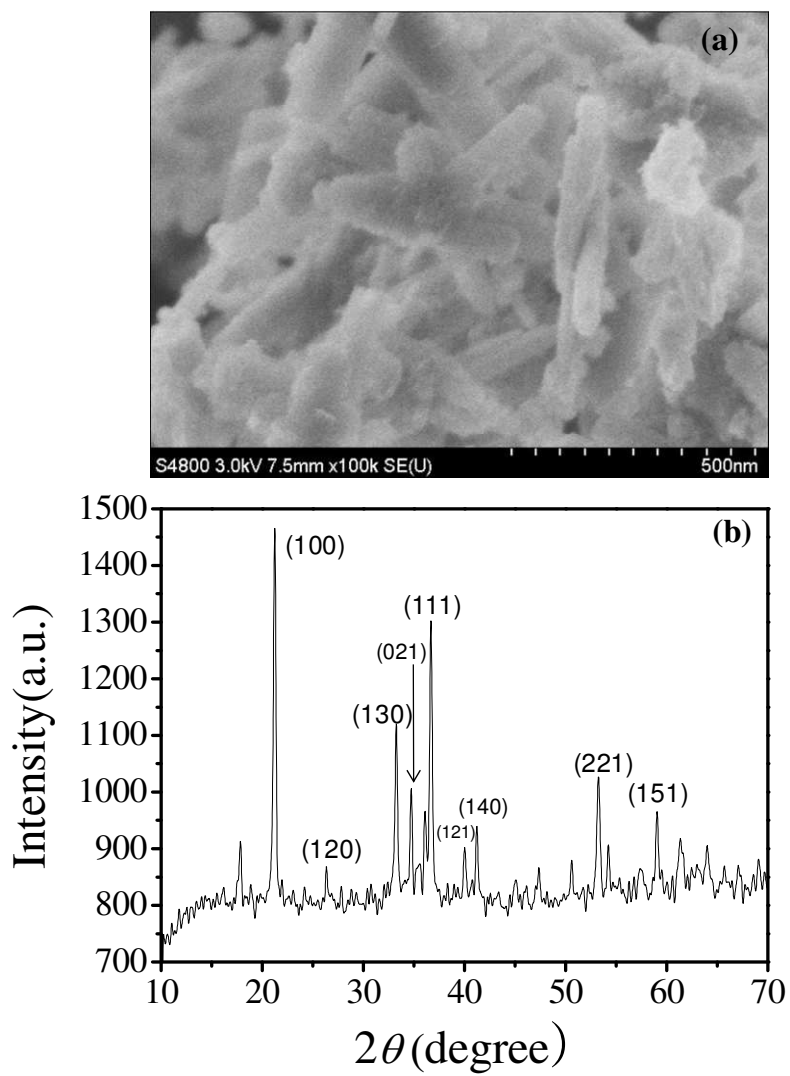


Fig. 1



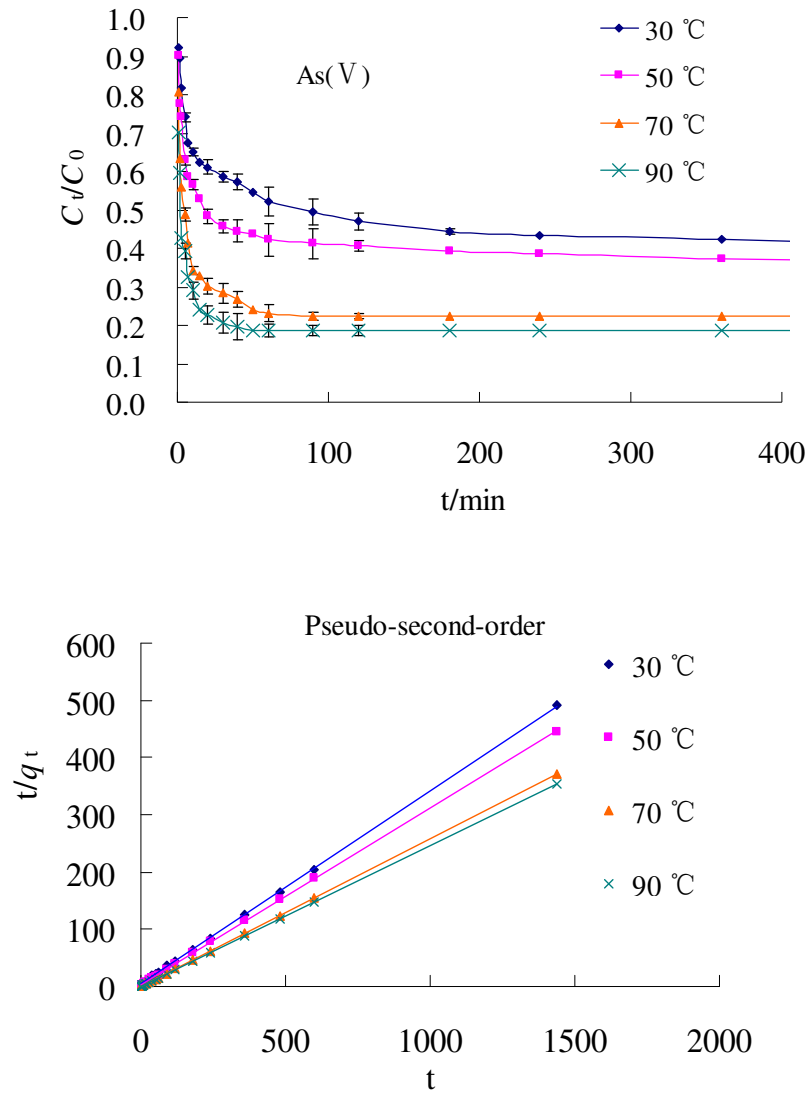


Fig. 2

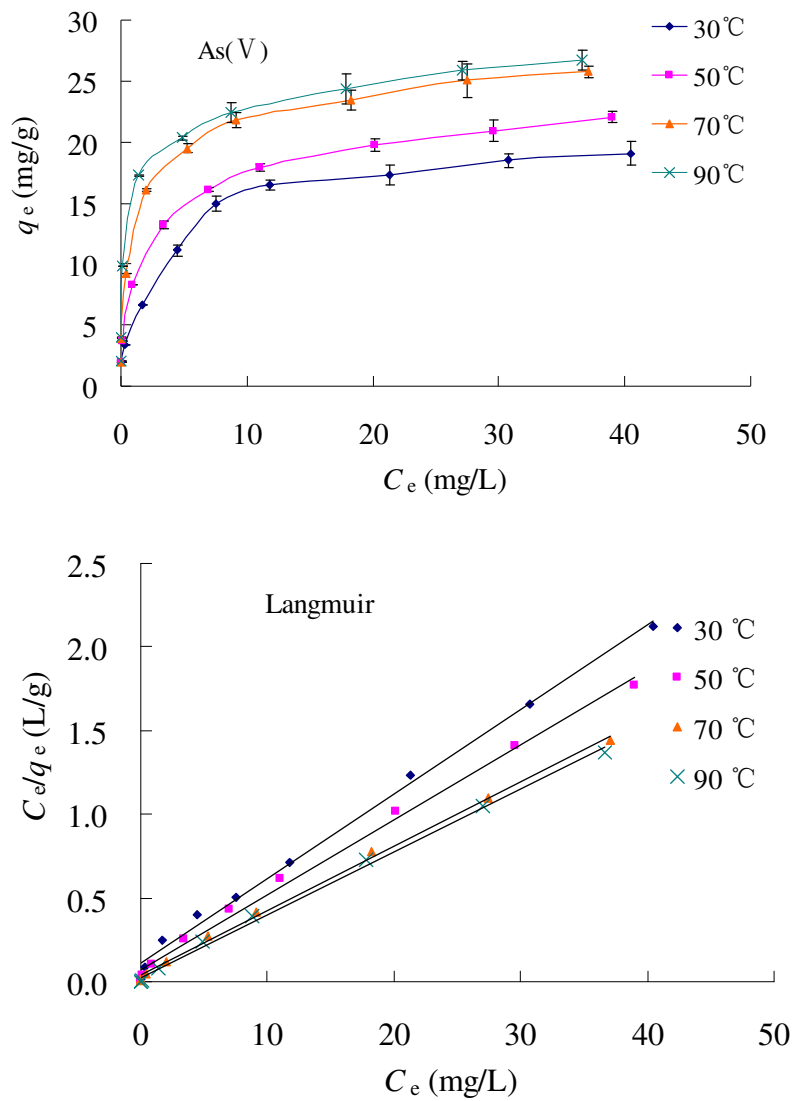


Fig. 3

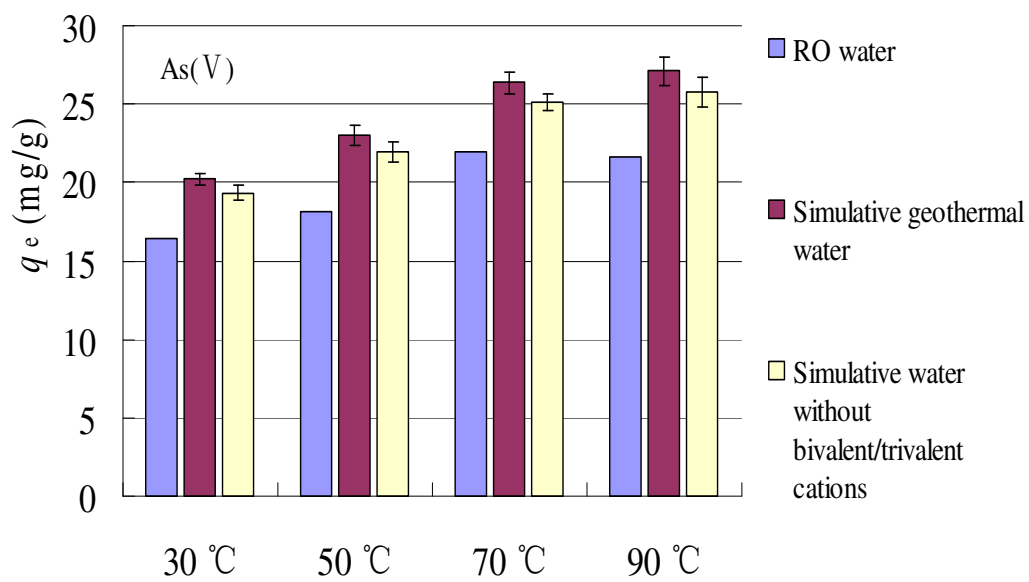


Fig. 4

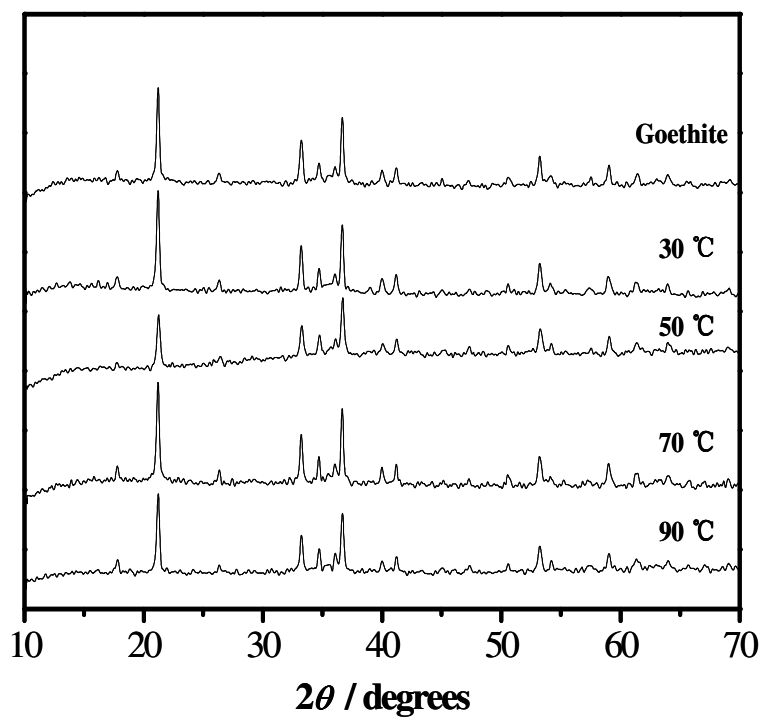


Fig. 5

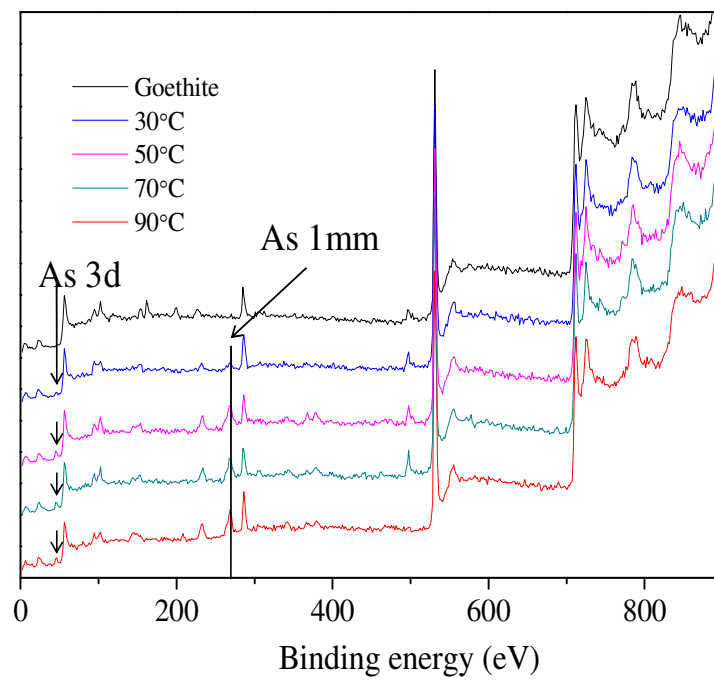


Fig. 6

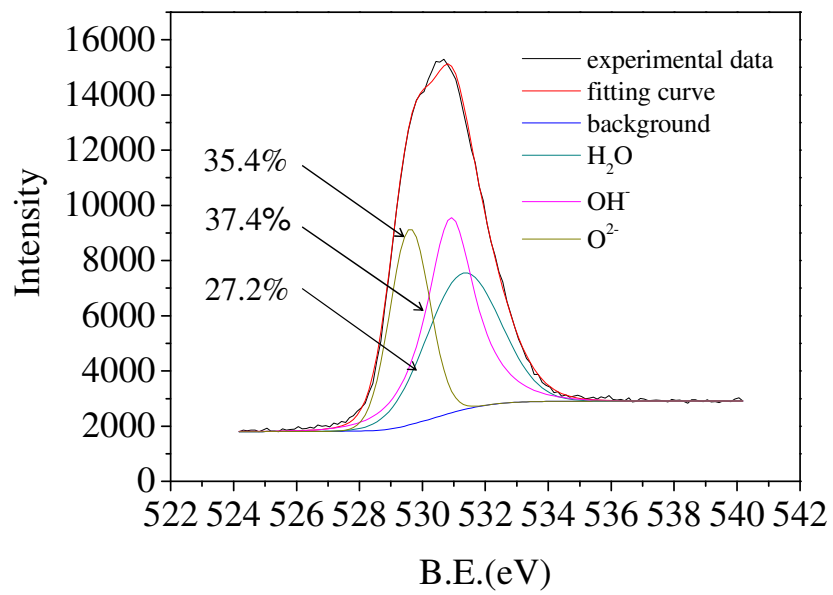


Fig. 7

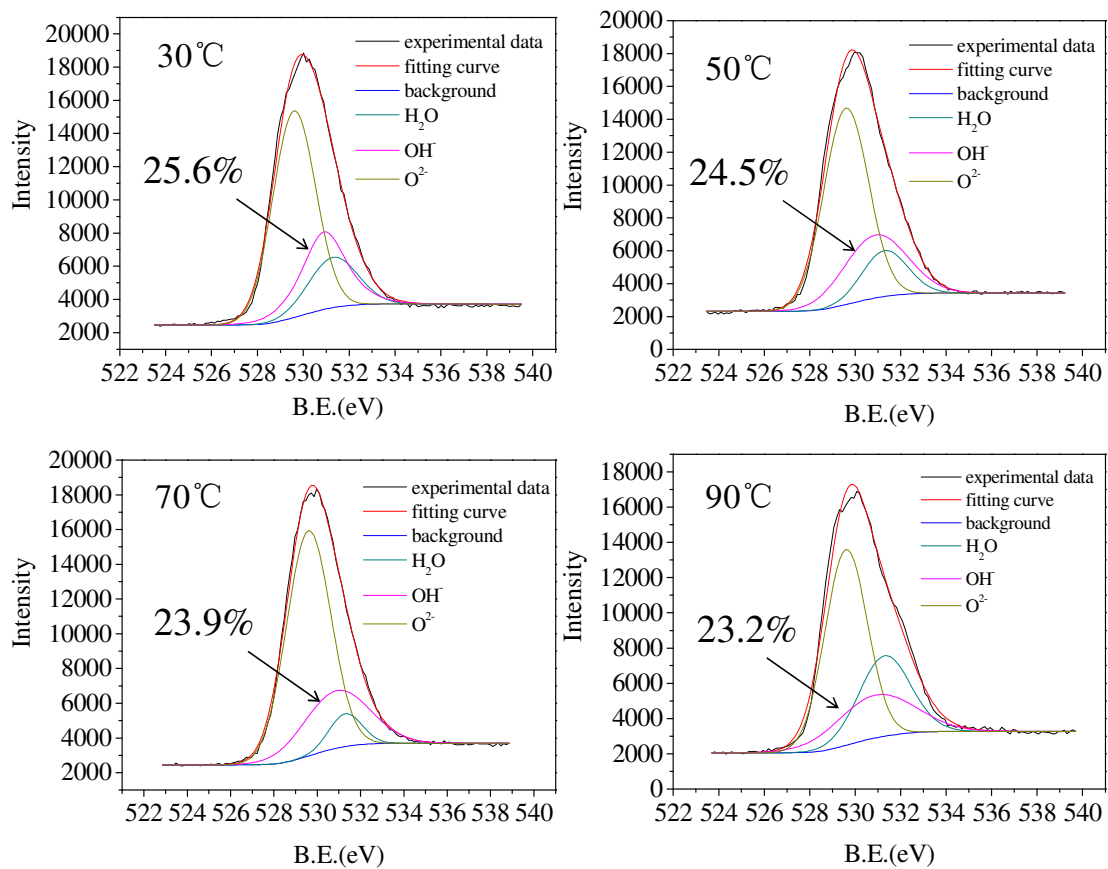


Fig. 8